

Supplementary Information:

Smartphone-Read Phage Lateral Flow Assay for Point-of-Care Detection of Infection

Maede Chabi,[†] Binh Vu,[‡] Kristen Brosamer,[†] Maxwell Smith,^{‡,¶} Dimple Chavan,^{§,||}
Jacinta C. Conrad,^{*,‡} Richard C. Willson,^{*,†,‡,§,⊥} and Katerina Kourentzi^{*,‡}

[†]Department of Biomedical Engineering, University of Houston, Houston, Texas 77204, USA

[‡]Department of Chemical and Biomolecular Engineering, University of Houston, Houston, Texas
77204, USA

[¶]Current address: Merck, Kenilworth, New Jersey 07033, USA

[§]Department of Biology and Biochemistry, University of Houston, Houston, Texas 77204, USA

^{||}Current address: Purification Process Sciences, BioPharmaceuticals Development, R&D,
AstraZeneca, Gaithersburg, Maryland 20878, USA

[⊥]Escuela de Medicina y Ciencias de Salud, Tecnológico de Monterrey, Monterrey, Nuevo León
64710, Mexico

*Corresponding author

E-mail: jcconrad@uh.edu; willson@uh.edu; edkourentzi@uh.edu

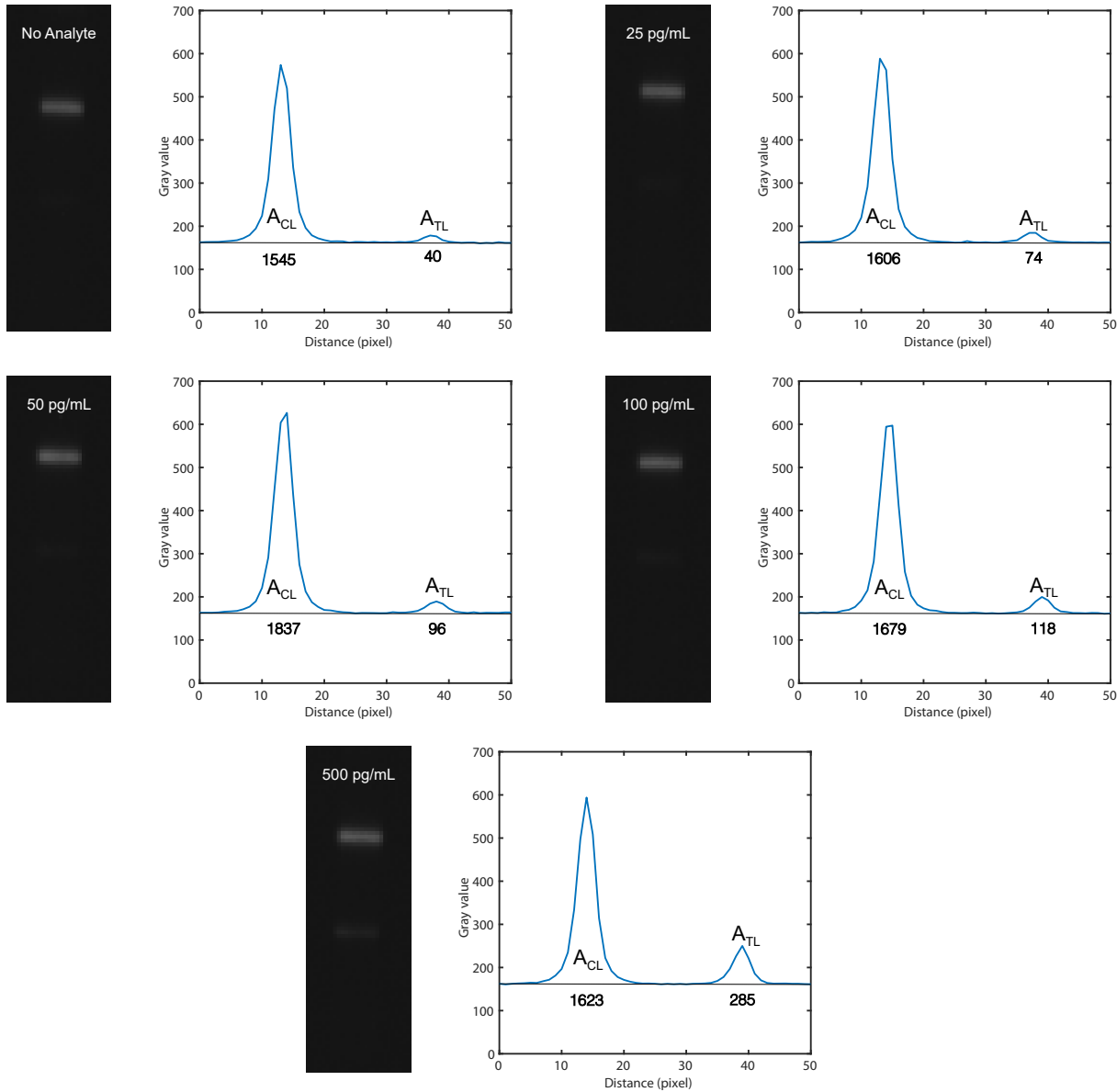


Figure S1: Typical negative (0 ng mL^{-1}) and a series of positive (25, 50, 100, 500 pg mL^{-1}) nucleoprotein in nasal swab extract) LFA strips imaged in grayscale on an AlphaInnotech FluorChem Gel Documentation system. Intensity profiles across the LFA strip length were extracted from the grayscale images using the plot profile tool of NIH ImageJ. To obtain the LFA TL/CL (A_{TL}/A_{CL}) ratio, the areas under the peaks on the intensity profile, A_{TL} and A_{CL} , were calculated. The integrated area of each peak is shown under the corresponding peak.

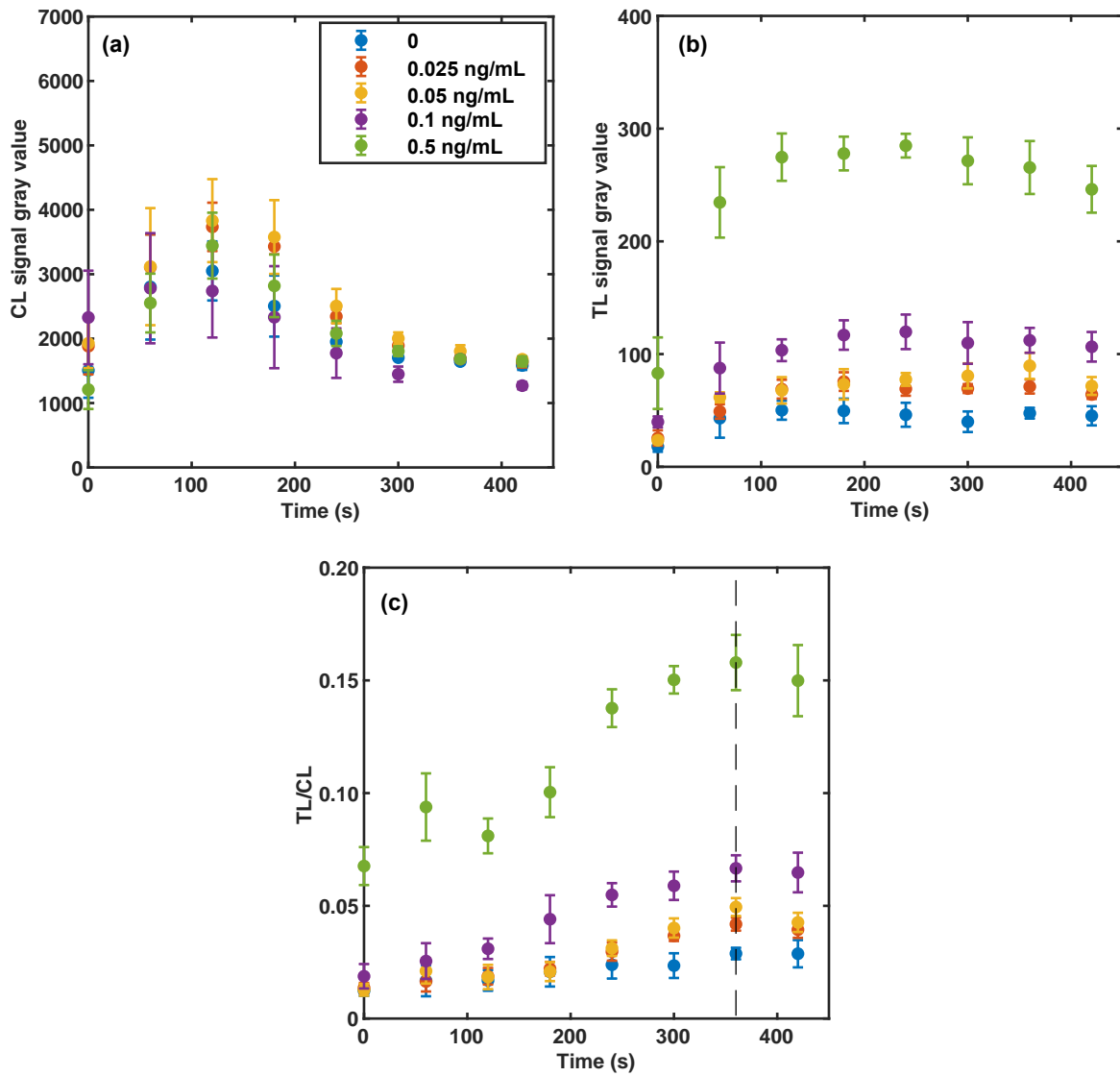


Figure S2: Temporal evolution of the phage LFA chemiluminescent signal (CL, TL and TL/CL). LFA strips were imaged repeatedly for 7 minutes using the FluorChem Gel Documentation system after dispensing the HRP substrate for 7 minutes. TL/CL ratios reached their maximum values at 6 minutes after adding the substrate (vertical dashed line). Error bars represent the standard deviation of four measurements. We estimated that there is approximately 10 s delay between (manual) application of the substrate, and initiating imaging after inserting the strips into the reader. As expected, given the high concentration of HRP enzymes on the CL, the individual signals, CL (a) and TL (b), do not increase at the same rate because there are many more HRP enzymes captured on the CL. TL/CL is mainly governed by changes in CL intensity and increases over time because of reduction in CL signal intensity. At 360 s, the TL, CL and TL/CL signals are stable to give a reliable read.

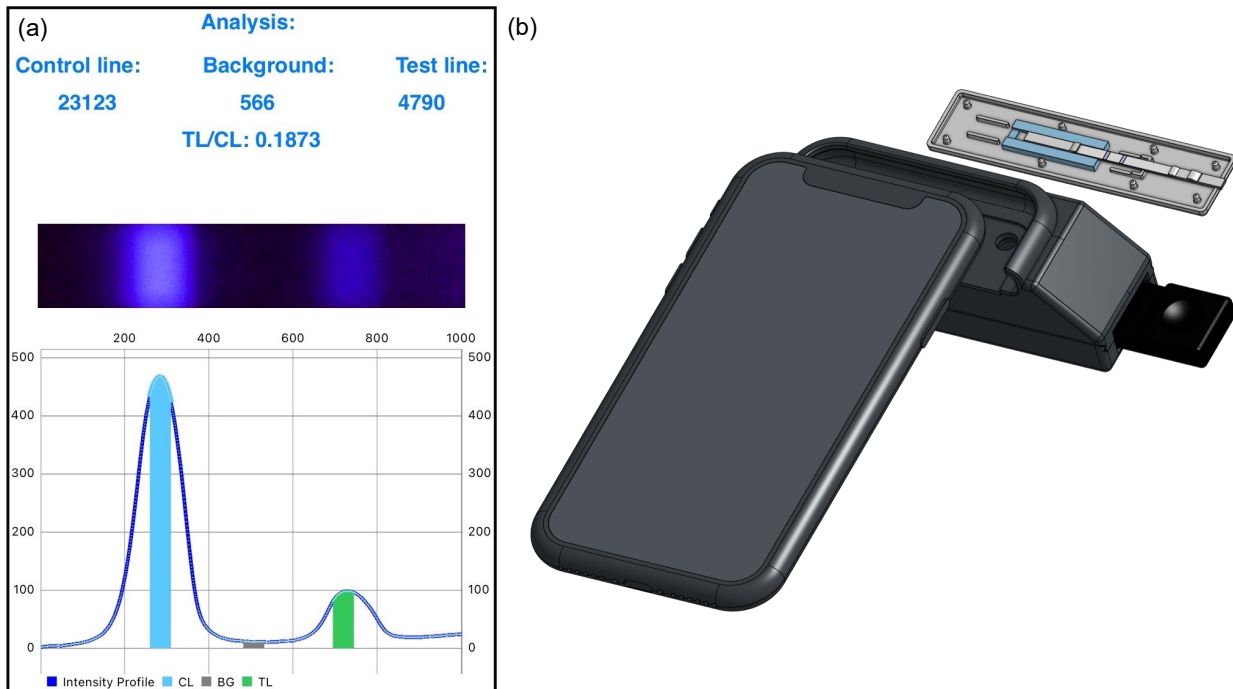


Figure S3: a) A typical analysis screen of the smartphone app after imaging a phage LFA strip. b) A 3-D illustration of the iPhone XR and the accessory attachment (in-house designed and coordinates made available at Thingiverse; <https://www.thingiverse.com/thing:5178342>) that holds the LFA cassette. The bottom part of the cassette where the LFA strip is placed is also shown. Despite the fact that different smartphone models will require different attachments, the attachment can be effortlessly re-designed to fit the specific requirements for imaging and the dimensions of the specific phone model and LFA cassette and thus it does not pose a significant barrier for adoption.

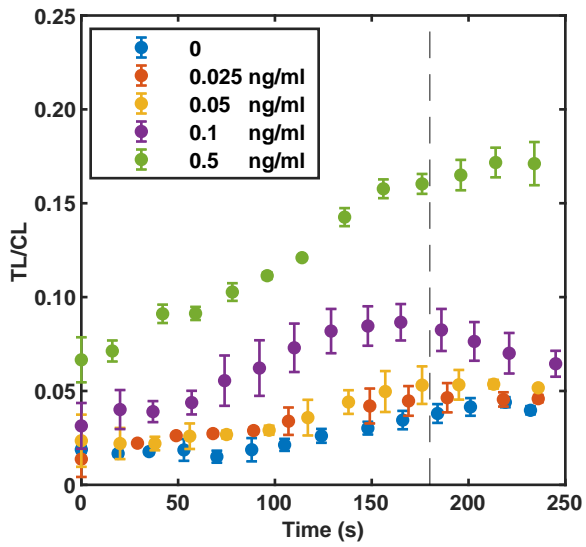


Figure S4: Temporal evolution of the chemiluminescent smartphone-read phage LFA. LFA strips were imaged using the smartphone starting around 3 s after dispensing the substrate onto the strips. Error bars represent the standard deviation of three measurements. We estimated that there is approximately 3 s delay between (manual) application of the substrate and initiating the imaging app after inserting the cassette into the smartphone accessory. TL/CL ratios for low nucleoprotein concentrations reached their maximum values around 3 minutes after adding the substrate (vertical dashed line) and this time was chosen as the standard reading time for the smartphone-imaged strips. The holder cassette, used only when reading the strips by smartphone, accelerates penetration of the ECL substrate into the membrane. This fact explains the difference in the timing of signal evolution when read with the smartphone (3 min) and the FluorChem system (6 min).

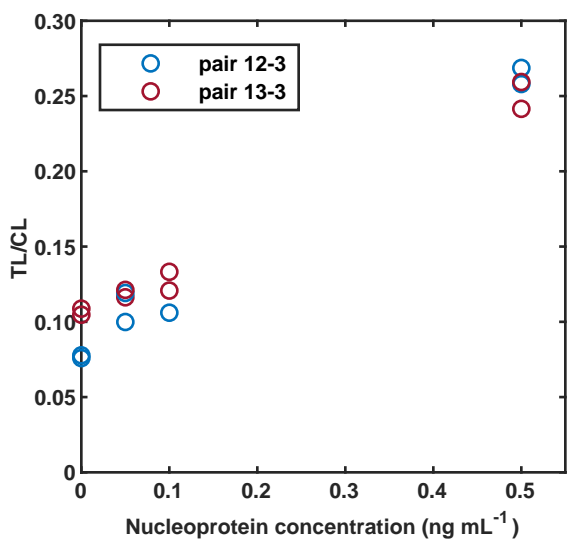


Figure S5: Titration curves for the two antibody pairs chosen after two rounds of screening (capture & detection antibodies: #12 & #3 and #13 & #3) using nasal swab extract spiked with recombinant nucleoprotein. All measurements are carried out in duplicate except for pair 12-3 at 0.1 ng mL⁻¹. The difference in background between Figure S5 and Figures 3 and 4 is a result of continuous improvements to the protocol during assay development. The data shown in Figure S5 (antibody screening) are from early experiments performed for reagent and method optimization during the initial development of the LFA.

Table S1: List of Labcorp frozen nasal swab extracts. The label “n.d.” indicates that the sample gave “not detected” Ct value in RT-PCR testing. These clinical samples were not tested on commercial rapid antigen tests due to the limited availability of those tests when we acquired the samples in the beginning of the pandemic.

| Index | Sample ID | Status | Ct value |
|-------|----------------|----------|----------|
| 1 | 813-COV-1004-0 | positive | 22.3 |
| 2 | 813-COV-1008-0 | positive | 24.9 |
| 3 | 813-COV-1009-0 | positive | 19.5 |
| 4 | 813-COV-1012-0 | positive | 24.7 |
| 5 | 813-COV-1014-0 | positive | 21.1 |
| 6 | 813-COV-1018-0 | positive | 26.4 |
| 7 | 813-COV-1022-0 | positive | 24.6 |
| 8 | 813-COV-1024-0 | positive | 22.7 |
| 9 | 813-COV-1025-0 | positive | 18.7 |
| 10 | 813-COV-1027-0 | positive | 26.2 |
| 11 | 813-COV-1028-0 | positive | 26.7 |
| 12 | 850-COP-1002-0 | positive | 29.1 |
| 13 | 850-COP-1003-0 | positive | 29.5 |
| 14 | 850-COP-1017-0 | positive | 27.7 |
| 15 | 850-COP-1022-0 | positive | 29.6 |
| 16 | 935-CON-1000-1 | negative | n.d. |
| 17 | 935-CON-1000-2 | negative | n.d. |
| 18 | 935-CON-1000-3 | negative | n.d. |
| 19 | 935-CON-1000-4 | negative | n.d. |
| 20 | 935-CON-1000-5 | negative | n.d. |
| 21 | 813-CON-2001-0 | negative | n.d. |
| 22 | 813-CON-2003-0 | negative | n.d. |
| 23 | 813-CON-2006-0 | negative | n.d. |
| 24 | 813-CON-2010-0 | negative | n.d. |
| 25 | 813-CON-2013-0 | negative | n.d. |
| 26 | 813-CON-2014-0 | negative | n.d. |
| 27 | 813-CON-2015-0 | negative | n.d. |

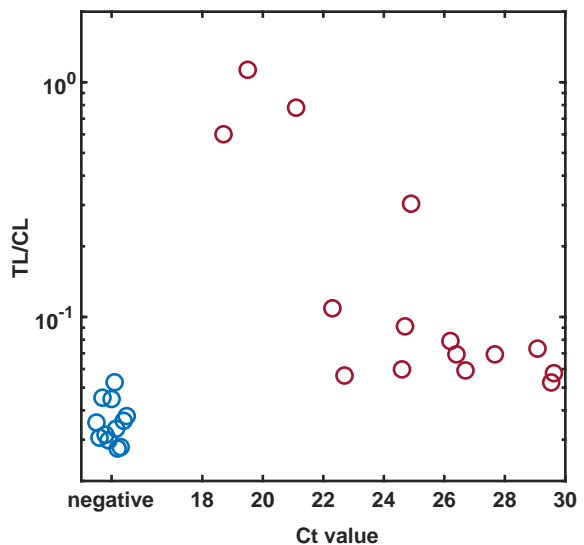


Figure S6: TL/CL ratios of phage LFA FluorChem-read of nasal swab extracts as a function of their Ct values.

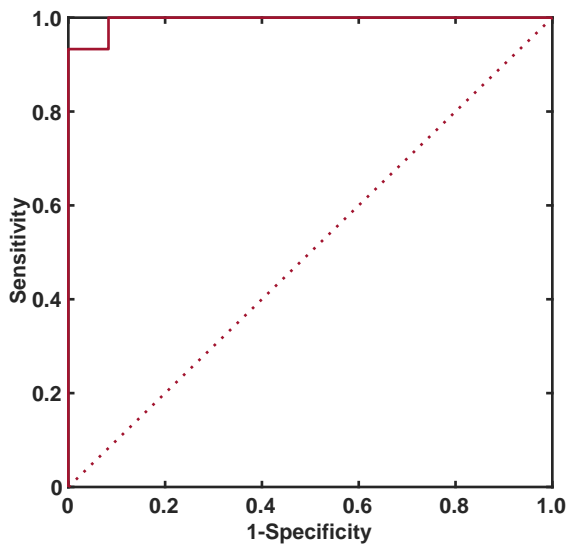


Figure S7: Receiver operating characteristic (ROC) curve for FluorChem read phage LFA. Based on the ROC analysis, we achieved a maximum sensitivity of 93.3% at 100% specificity. The area under the ROC curve (AUC) was 0.994 with a 95% confidence interval of 0.977–1.00. We note, however, that significantly more samples would be required to reliably assess the clinical performance of the technology.

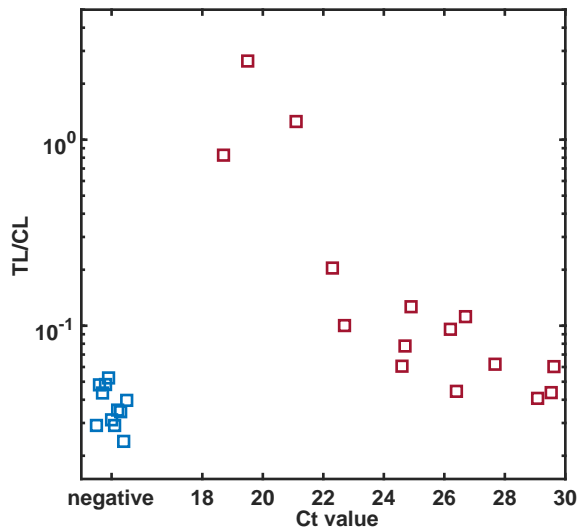


Figure S8: TL/CL ratios of Smartphone-read phage LFA of nasal swab extracts as a function of their Ct values.

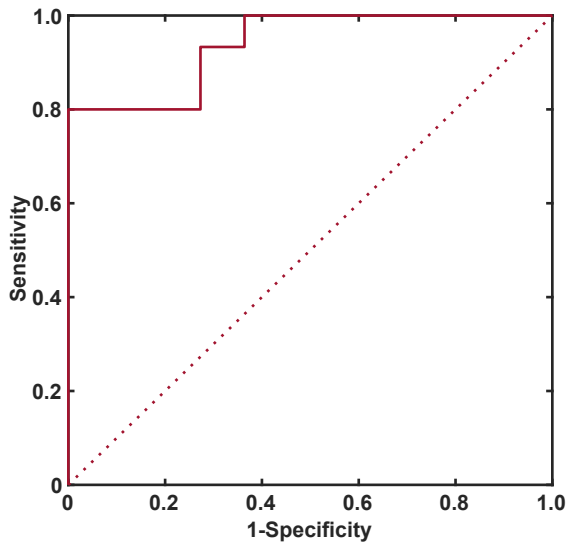


Figure S9: Receiver operating characteristic (ROC) curve for smartphone read phage LFA. Based on the ROC analysis, we achieved a maximum sensitivity of 80% at 100% specificity. The area under the ROC curve (AUC) was 0.939 with 95% confidence interval of 0.854–1.00. We note, however, that significantly more samples would be required to reliably assess the clinical performance of the technology.

Cost estimation

Both gold and phage reporters are small components of the total manufacturing and packaging costs of LFAs. We estimate the cost of phage particles at 0.0005 USD per test (plus 0.001

USD per test for the HRP-antibody conjugate); the cost of (carboxylated) gold nanoparticles (Nanocomposix) is estimated at 0.018 USD per test. The cost of the chemiluminescent substrate is estimated at 0.030 – 0.035 USD per test. These price estimates are based on the retail price for small-scale orders and the prices can be much lower for bulk orders towards commercialization. Thus, the cost of the reporters is negligible in comparison to other production costs for a commercialized LFA.

Table S2: Limit of Detection (LoD) of recently published SARS-CoV-2 antigen LFAs.

| reporter | target | limit of detection * | clinical samples | readout | reference |
|--|-----------------------------|--|------------------------|--------------------------------------|-----------------------------|
| gold nanoparticles | N protein | 250 pg mL ⁻¹ | nasopharyngeal samples | visual | Mertens et al. ¹ |
| gold nanoparticles (copper deposition) | S protein N protein | 1 ng mL ⁻¹ 0.1 ng mL ⁻¹ | masopharyngeal swabs | visual | Liu et al. ² |
| gold nanoparticles (thermal contrast amplification (TCA)) | RBD | 10 pg mL ⁻¹ [†] | no | visual | Peng et al. ³ |
| gold nanoparticles | RBD | 1 fg mL ⁻¹ [†] | nasopharyngeal swabs | visual | Liu et al. ⁴ |
| latex particles | S protein N protein | TCA: 0.125 fg mL ⁻¹ [†] | laser/IR detector | visual | Baker et al. ⁵ |
| cellulose nanobeads | N protein | 5 µg mL ⁻¹ | no | visual | Grant et al. ⁶ |
| cellulose nanobeads | S1 protein RBD | 650 pg mL ⁻¹ 20 ng mL ⁻¹ [†] | no | visual | Kim et al. ⁷ |
| quantum dots | N protein | 50 ng mL ⁻¹ [†] | nasopharyngeal swabs | visual | Lee et al. ⁸ |
| magnetic quantum dots | S protein N protein | 10 ng mL ⁻¹ [†] | swabs | visual | |
| latex beads | gamma irradiated SARS-CoV-2 | 5 pg mL ⁻¹ [†] | no | fluorescent reader | Wang et al. ⁹ |
| Co-Fe@hemin-peroxidase nanozyme | S-RBD pseudovirus | 0.5 pg mL ⁻¹ [†] 0.5 pg mL ⁻¹ [†] | no | fluorescent reader | Wang et al. ¹⁰ |
| antibody-HRP phage (chemiluminescent) | N protein | 4 TCID50/swab [‡] (2.5x10 ⁴ copies/swab) | no | visual | Grant et al. ¹¹ |
| | | 100 pg/mL 360 TCID50/mL | no | smartphone imaging computer software | Liu et al. ¹² |
| | | | | image analysis | present study |
| | | | | off-the-shelf smartphone | |

* based on analyte spiked in buffer or otherwise noted

[†] based on analyte spiked in clinical matrix[‡] based on analyte spiked in simulated respiratory secretion (SRS)

References

- (1) Mertens, P. et al. Development and Potential Usefulness of the COVID-19 Ag Respiratory Strip Diagnostic Assay in a Pandemic Context. *Front. Med.* **2020**, *7*, 225.
- (2) Liu, D.; Wu, F.; Cen, Y.; Ye, L.; Shi, X.; Huang, Y.; Fang, S.; Ma, L. Comparative research on nucleocapsid and spike glycoprotein as the rapid immunodetection targets of COVID-19 and establishment of immunoassay strips. *Mol. Immunol.* **2021**, *131*, 6–12.
- (3) Peng, T.; Jiao, X.; Liang, Z.; Zhao, H.; Zhao, Y.; Xie, J.; Jiang, Y.; Yu, X.; Fang, X.; Dai, X. Lateral Flow Immunoassay Coupled with Copper Enhancement for Rapid and Sensitive SARS-CoV-2 Nucleocapsid Protein Detection. *Biosensors* **2022**, *12*, 13.
- (4) Liu, Y.; Zhan, L.; Shen, J. W.; Baro, B.; Alemany, A.; Sackrison, J.; Mitjá, O.; Bischof, J. C. fM-aM Detection of the SARS-CoV-2 Antigen by Advanced Lateral Flow Immunoassay Based on Gold Nanospheres. *ACS Appl. Nano Mater.* **2021**, *4*, 13826–13837.
- (5) Baker, A. N. et al. The SARS-CoV-2 Spike Protein Binds Sialic Acids and Enables Rapid Detection in a Lateral Flow Point of Care Diagnostic Device. *ACS Cent. Sci.* **2020**, *6*, 2046–2052.
- (6) Grant, B. D.; Anderson, C. E.; Williford, J. R.; Alonzo, L. F.; Glukhova, V. A.; Boyle, D. S.; Weigl, B. H.; Nichols, K. P. SARS-CoV-2 Coronavirus Nucleocapsid Antigen-Detecting Half-Strip Lateral Flow Assay Toward the Development of Point of Care Tests Using Commercially Available Reagents. *Anal. Chem.* **2020**, *92*, 11305–11309.
- (7) Kim, H.-Y.; Lee, J.-H.; Kim, M. J.; Park, S. C.; Choi, M.; Lee, W.; Ku, K. B.; Kim, B. T.; Park, E. C.; Kim, H. G.; Kim, S. I. Development of a SARS-CoV-2-specific

- biosensor for antigen detection using scFv-Fc fusion proteins. *Biosens. Bioelectron.* **2020**, *175*, 112868.
- (8) Lee, J.-H.; Choi, M.; Jung, Y.; Lee, S. K.; Lee, C.-S.; Kim, J.; Kim, J.; Kim, N. H.; Kim, B.-T.; Kim, H. G. A novel rapid detection for SARS-CoV-2 spike 1 antigens using human angiotensin converting enzyme 2 (ACE2). *Biosens. Bioelectron.* **2021**, *171*, 112715.
- (9) Wang, C.; Yang, X.; Zheng, S.; Cheng, X.; Xiao, R.; Li, Q.; Wang, W.; Liu, X.; Wang, S. Development of an ultrasensitive fluorescent immunochromatographic assay based on multilayer quantum dot nanobead for simultaneous detection of SARS-CoV-2 antigen and influenza A virus. *Sens. Actuators B Chem.* **2021**, *345*, 130372.
- (10) Wang, C.; Cheng, X.; Liu, L.; Zhang, X.; Yang, X.; Zheng, S.; Rong, Z.; Wang, S. Ultrasensitive and Simultaneous Detection of Two Specific SARS-CoV-2 Antigens in Human Specimens Using Direct/Enrichment Dual-Mode Fluorescence Lateral Flow Immunoassay. *ACS Appl. Mater. Interfaces* **2021**, *13*, 40342–40353.
- (11) Grant, B. D.; Anderson, C. E.; Alonzo, L. F.; Garing, S. H.; Williford, J. R.; Baughman, T. A.; Rivera, R.; Glukhova, V. A.; Boyle, D. S.; Dewan, P. K.; Weigl, B. H.; Nichols, K. P. A SARS-CoV-2 coronavirus nucleocapsid protein antigen-detecting lateral flow assay. *PLoS ONE* **2021**, *16*, e0258819.
- (12) Liu, D.; Ju, C.; Han, C.; Shi, R.; Chen, X.; Duan, D.; Yan, J.; Yan, X. Nanozyme chemiluminescence paper test for rapid and sensitive detection of SARS-CoV-2 antigen. *Biosens. Bioelectron.* **2021**, *173*, 112817.